Research Article / Systems and Computer Engineering https://doi.org/10.15446/ing.investig.90748

# An Automatic Approach for Bone Tumor Detection from Non-Standard CT Images

## Un enfoque automático para la detección de tumores óseos a partir de imágenes de CT no estándar

Hatice Catal Reis[1] and Bulent Bayram[2]

**ABSTRACT**

Image processing techniques are applied in many fields of science. This study aims to detect tumors in the foot and create 3D models via computed tomography (CT), as well as to produce biometric data. 1 039 CT images were obtained from a server. The parameters used were a collimation of 64 detectors, a scanning thickness of 0,5-3 mm, and a pixel size of 512 x 512, with a radiometric resolution of the 16-bit gray levels. Noise reduction, segmentation, and morphological analysis were performed on CT scans to detect bone tumors. In addition, this study used digital image processing techniques to create a virtual three-dimensional (3D) model of bone tumors. The performance of our proposal was evaluated by analyzing the receptor operating characteristics (ROC). According to the results, the sensitivity, specificity, and precision in tumor detection were 0,96, 1, and 0,98%, respectively, with a 0,99% average F-measure. Radiologist reports were used for the sake of comparison. The proposed technique for detecting bone tumors of the foot via CT can help radiologists with its increased precision, sensitivity, specificity, and F-measure. This method could improve the diagnosis of foot and ankle tumors by allowing for the multidirectional quantification of abnormalities.

**Keywords:** CT, medical image processing, region-growing algorithm, bone tumor, 3D

**RESUMEN**

Las técnicas de procesamiento de imágenes se aplican en muchos campos de la ciencia. El objetivo de este estudio es detectar tumores en el pie y crear modelos 3D mediante tomografía computarizada (CT), así como producir datos biométricos. 1 039 imágenes de CT se obtuvieron de un servidor. Los parámetros utilizados fueron una colimación 64 detectores, un grosor de escaneo de 0,5-3 mm y un tamaño del píxel de 512 x 512, con una resolución radiométrica de niveles de gris de 16 bits. Se realizó reducción de ruido, segmentación y análisis morfológico a imágenes CT para detectar tumores óseos. Adicionalmente, en este estudio se aplicaron técnicas de procesamiento de imágenes digitales para crear un modelo virtual tridimensional (3D) de tumor óseo. El rendimiento de nuestra propuesta se evaluó con base en el análisis de las características operativas del receptor (ROC). Según los resultados, la sensibilidad, la especificidad y la precisión en la detección de tumores fue de 0,96, 1 y 0,98 % respectivamente, con un F-*measure* promedio de 0,99 %. Se utilizaron reportes de radiología para efectos de comparación. La técnica propuesta para detectar tumores óseos del pie mediane CT puede ayudar a los radiólogos dada su alta precisión, sensibilidad, especificidad y F-*measure*. Este método puede mejorar el diagnóstico de tumores de pie y tobillo al permitir la cuantificación multidireccional de anomalías.

**Palabras clave:** CT, procesamiento de imágenes médicas, algoritmo de crecimiento de regiones, tumor óseo, 3D

**Received:** September 25th, 2020
**Accepted:** February 17th, 2023

## Introduction

Photogrammetry involves scientific methods that calculate an object's 3D coordinates using overlays of two consecutive images (Akcay *et al*., 2017). It is frequently used in fields such as forestry, agriculture, environment, mining, planning, and medicine. Medical photogrammetry can precisely present an organ's metric and morphometric measurements and location data without making contact with the patient or the organ (Catal Reis, 2018). Medical photogrammetry using medical data can detect anomalies and cancer. Cancer occurs due to various environmental and genetic factors. The most prevalent types amount to over 100 different known cancers, such as skin cancer (Parker, 2020), lung cancer (Plodkowski *et al*., 2021), prostate cancer (Ghafouri-Fard *et al*., 2020), melanoma (Esim *et al*., 2019), stomach cancer (Zilberman *et al*., 2015), breast cancer (Riis, 2020), bone cancer (Hosseini *et al*., 2020), *etc*. Bone tumors are more widespread in adults than in children and youngsters (Reddy *et al*., 2015). Tumors and tumor-like lesions of the foot and ankle are rare (Toepfer, 2017; Foo and Raby, 2005; Bakotic and Huvos, 2001). Foot tumors have about a 3% ratio among all skeletal tumors (Yan *et al*., 2018). Benign bone tumors are more common than malignant primary bone tumors in the foot (Ozer *et al*., 2017). However, benign bone tumors are generally asymptomatic and go unexplored (Ladd and Roth,

[1] PhD in Geomatics Engineering, Yildiz Technical University, Turkey. Affiliation: Assistant professor, Department of Geomatics Engineering, Gumushane University, Gumushane, Turkey. E-mail: hatice.catal@yahoo.c-om.tr

[2] PhD in Geomatics Engineering, Yildiz Technical University, Turkey. Affiliation: Professor, Department of Geomatics Engineering, Yildiz Technical University, Istanbul, Turkey. E-mail: bulentbayram65@gmail.com

Attribution 4.0 International (CC BY 4.0) Share - Adapt

2017). A tumor is the abnormal development of new cells that may occur in any of the body parts (Mistry *et al*., 2016).

The most often faced primary benign bone tumor of the foot is the unicameral bone cyst (UBC), found in second osteochondroma and osteoid osteoma. Calcaneus tumors are especially rare; 32% of them are benign, and 35% of osseus tumor types occur in the foot (Young *et al*., 2013). Calcaneus tumors are the second most common condition involving the foot after meta-tarsals (Kilgore and Parrish, 2005). However, accurately and reliably describing and quantifying foot tumors is a challenging task for orthopedic surgeons and orthopedists. Bone anomalies in the foot and ankle are complex structures and, therefore, difficult to quantify by standard radiographic measurements. The literature is limited to calcaneus lesions. In particular, studies of calcaneus tumors consist of case reports describing a single primary tumor of the calcaneus (Yan *et al*., 2018). The first significant cases related to calcaneus tumors and tumor-like conditions were described in 1973 by Campbell and Leupold. These authors presented a case of a rare elastofibroma (soft tissue tumor) in the calcaneus of a 79-year-old female (Pirak *et al*., 2020). Another case of a giant cell tumor of the calcaneus with a bone cyst was reported by Kamal *et al*. (2016). The case of a 21-year-old male patient with osteosarcoma of the calcaneus was presented by Diémé *et al*. (2015). Past and present research has focused on classifying tumor types, growth directions, and areas, as well as on determining locations (Costelloe and Madewell, 2013). Foo and Raby (2005) presented the spectrum of tumors and tumor-like lesions of the foot and ankle which are not considered standard. Since calcaneal tumor types are rare, delays in diagnosis, incorrect diagnosis, and unnecessary amputations can be observed (Young *et al*., 2013).

Several diagnosis methods have been proposed for tumor detection. However, radiological images are the gold standard and primary step for tumor evaluation (Ladd and Roth, 2017; Bestic *et al*., 2020). Magnetic Resonance Imaging (MRI) and Computed Tomography (CT) are commonly used for diagnosis (Hasbek *et al*., 2013; Gemescu *et al*., 2019; Scotto di Carlo *et al*., 2020). High spatial-resolution CT supplies sensitive bone details, thus making it a vital tool in various cases and with specific tumors (Ladd *et al*., 2017; Mehta *et al*., 2017). CT scans are better at evaluating bone tumors for destruction or breakthrough than MR imaging (Hapani *et al*., 2014). When a tumor metastasizes to the bone, severe pain and deterioration occur on it, considerably reducing the possibility of a treatment (Weilbaecher *et al*., 2011). A significant limitation for studying what regulates tumors in the bone is the lack of non-contact models for tumor reconstruction, as well as the limited ability to detect low tumor levels in the bone. In addition, low-resolution and noisy images may prevent the tumor from being easily detected and are time-consuming. There needs to be more tools in addition to these imaging and diagnosis systems in order to obtain accurate and reliable results. A second opinion is essential to meet the requirements of imaging systems and mitigate the possible failures of technicians and physicians. Therefore, photogrammetry and medical image processing are the best techniques for using non-standard CT images, as they produce highly accurate results. Image processing technology converts data into different formats, and it is useful for measuring and evaluating (Aydın and Kurnaz, 2023). Therefore, Computer-Aided Diagnostics (CAD) has been proposed for diagnosis and treatment (Lodwick *et al*., 1963). Today, techniques for 3D bone measurement have become available (Qiang *et al*., 2014), which allow for surface, distance, location, and angular measurements on models generated from CT or MRI images (Gutekunst *et al*., 2013; Eckstein *et al*., 2006).

Many CAD methods have already been employed, including 2D and 3D approaches for tumor measurement (Nishikawa, 2005). However, little data are currently available in the literature with regard to measuring the 3D morphological parameters of the calcaneus (Qiang *et al*., 2014).

This study aims to evaluate the feasibility of medical photogrammetry for the detection of bone tumors, with the purpose of automatically detecting calcaneus tumors in noisy, non-standard CT images, as well as visualizing them in 3D and evaluating their metric information. CT images were used in this study, and the tumor segmentation and 3D model were created using software. This research provides an overview of the evidence for using CAD with calcaneus tumors. This highly sensitive method to detect bone tumors is ultimately summarized regarding its applicability to each foot tumor model. Medical image processing to detect foot tumors in CT can assist radiologists by increasing their accuracy. The proposed techniques to detect small and significant changes in tumors and tumor-like lesions, combined with these novel models, will be instrumental in studying tumors in the bone (benign or metastatic), as well as their stages.

Our study comprises three sections. The next section characterizes the calcaneus and explains the dataset. Then, general information is presented regarding medical image processing (pre-processing, segmentation, 3D modeling, obtaining biometric information, and statistical analysis). Afterwards, the results are presented and discussed while making a set of recommendations. The final section deals with the conclusions of this work.

## Materials and methods

In medical imaging, conversion from 2D to 3D or *vice versa* can be done with the help of photogrammetric techniques. The length, area, volume, and geometric information can be accessed by processing these data. In addition, contactless information and metric data can be obtained through metric measurements (Doğan and Yakar, 2018). This study focuses on tumor detection in the calcaneus bone via the medical photogrammetric approach.

The calcaneus bone is the largest tarsal bone and is irregularly shaped, with complex edges and articular surfaces (Qiang *et al.*, 2014). It is a large bone that forms the base of the back of the foot. The calcaneus 'cuboid' connects bones and the talus. The bond between the talus and the calcaneus forms sub-articular joints. This joint is essential for normal foot function (Epstein *et al.*, 2012; Basile *et al.*, 2012).

As for this study, from 2011 to 2014, 20 cases (left and right foot scans) were taken from the server (retrospective study/stock footage research), for a total of 1 039 CT scans. The foot and ankle CT images of 10 cases (male group age: 20,2±9,8; female group age: 47±31) were included given the presence of calcaneal bone tumors and tumor-like-lesions. The imaging procedures were carried out according to the Helsinki Declaration (Goodyear *et al.*, 2007). This study did not require ethical approval or informed consent by national legislation.

CT images were taken from an open-access public hospital database. The medical photogrammetry and digital medical image format used was DICOM (Digital Imaging and Communications in Medicine). Most commercial software applications support the .dcm format, which facilitates reading raw data and sharing them. Therefore, DICOM has become a standard format for medical imaging. The parameters employed were a detector collimation of 64, a scanning thickness of 0,5-3 mm, and pixel sizes of 512 x 512, with a radiometric resolution of 16-bit gray levels (Table 1). Package software was used (Able Software Corp., USA) for 3D modelling and biometric data, as well as MATLAB for pre-processing and statistical analysis. All this, on a computer with an Intel Core i7-2670QM duo processor @2.20 GHz and 6 GB RAM. The axial images (.dcm) were first transferred into a personal computer with the 3D modeling software used in this study. Calibration was performed automatically.

**Table 1.** Imaging parameters for CT scanning

| Patient Name | Gender | Scanning thickness | Number of slices | Age | Tube current (mA) Tube voltage (kV) |
|---|---|---|---|---|---|
| **1** | Male | 2 mm | 85 | 19 | 100-120 |
| **2** | Female | 3 mm | 59 | 13 | 100-120 |
| **3** | Female | 2 mm | 85 | 53 | 100-120 |
| **4** | Female | 0,5 mm | 313 | 48 | 100-120 |
| **5** | Female | 2 mm | 101 | 43 | 100-120 |
| **6** | Male | 2 mm | 81 | 14 | 100-120 |
| **7** | Male | 2 mm | 88 | 30 | 100-120 |
| **8** | Female | 2 mm | 81 | 78 | 100-120 |
| **9** | Male | 2 mm | 76 | 20 | 100-120 |
| **10** | Male | 2 mm | 70 | 18 | 100-200 |

**Source:** Authors

Figure 1 shows a diagram of the proposed architecture, which consists of seven different processes.

This study followed these steps: (1) image pre-processing, (2) calcaneus segmentation, (3) tumor segmentation, (4) 3D modeling – visualization, and (5) biometric calculation. These five steps make up the primary process, in comparison with the seven steps of the physician report.

Our study involved the processing of bone CT images, so as to identify the region of bone cancer and perform a 3D evaluation. Axial raw CT images containing healthy and bone tumors are presented in Figures 2 and 3.

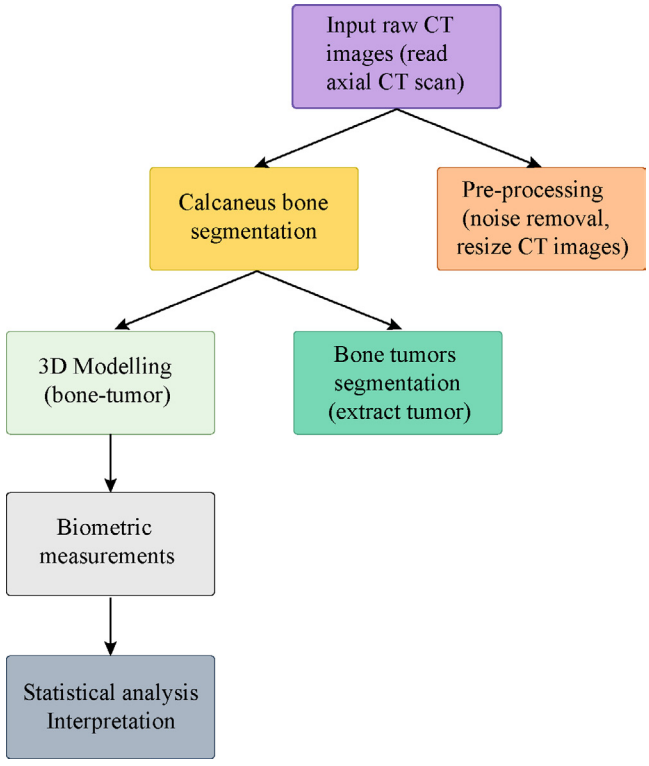


**Figure 1.** Schematic diagram of the workflow
**Source:** Authors

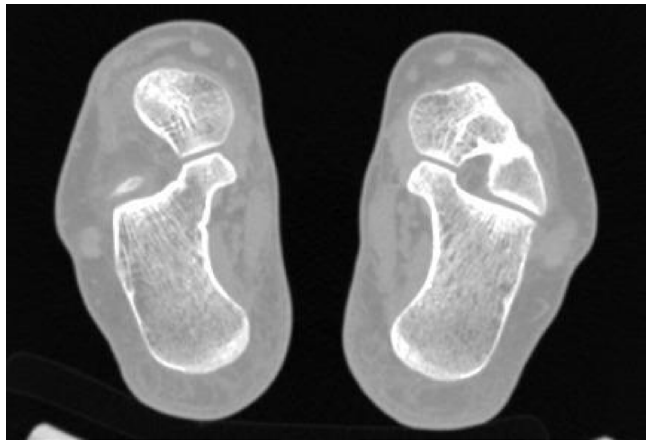

**Figure 2.** Axial CT image of a healthy person
**Source:** Authors

The calcaneus CT images employed were noisy images of various sizes. Image pre-processing can improve the accuracy of a 3D model. To this effect, data selection and classification (tumor or non-tumor) were performed, followed by a resizing of the CT images, which were

discarded if there was still noise. The most important goal here was to sort out images of different diseases. Another critical point was using noise removal techniques to enhance the images (the noise outside the main calcaneus bone was removed). Therefore, the images were pre-processed.


**Figure 3.** (A, B, C) axial CT slices of bone tumors
**Source:** Authors

In a classification process, the pixels of an image are segmented based on determining features. Segmentation methods and their success rates can vary according to their aim, applied field, and the quality of the image used. In general, segmentation algorithms are dependent on discontinuity and the similarity of grey levels (González and Woods, 2007).

A region-growing algorithm was applied to find the Region of Interest (ROI) of foot bone tumors. This method searches for similarities in the grey levels of an image for segmentation (Figure 4). It is important for the sets created here to be homogeneous, which does not depend on the training process. Although different region-growing algorithm approaches have been developed and proposed, the main general steps of the method can be ordered as thresholding, growing, and split-merge (González and Woods, 2007). This method grows from seeds to adjacent points via thresholding techniques.

Data were collected from the Hounsfield Units of the images to establish a suitable threshold value for the region membership criterion. Tumor segmentation and 3D tumor models were created via commercial software.

Afterwards, a 3D model was created from the segmented images. The performance of this model was evaluated in terms of its accuracy in the segmentation of the calcaneus CT images. Using the region-growing algorithm to extract the correct edge contour increased the performance of the study. Then, biometrical calculations were performed. The steps for image processing consisted of noise reduction, resizing, segmentation, 3D modeling, and morphological analysis.

To summarize this study's workflow, the CT image was read, pre-processed, segmented and edited; a 3D model was generated; and biometric measurements were performed. The tumor location is illustrated in Figure 5.

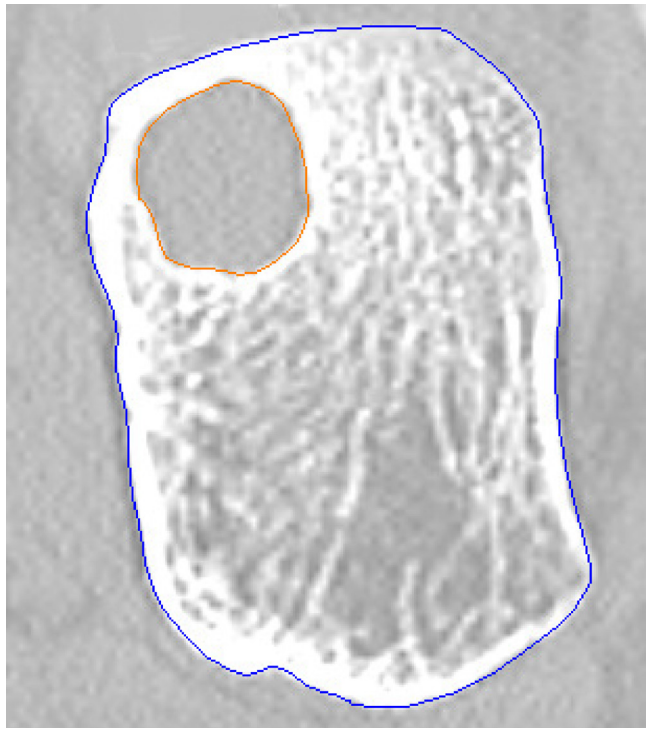

**Figure 4.** Segmentation result of the calcaneus bone and its tumor using CT
**Source:** Authors

**Figure 5.** 3D morphological measurements of the calcaneus and the location of tumors in it (orange denotes a tumor, and blue is the calcaneus body)
**Source:** Authors

### *Statistical analysis*

The morphological parameters of the 3D measurements were evaluated using statistical analysis. The performance of the study was evaluated with receiver operating characteristic (ROC) analysis. The parameters are the following: true positive (TP), false negative (FN), true negative (TN), and false positive (FP) (Nahm, 2022). The area under the ROC curve (AUC= 0,5) (Nurtanio *et al.*, 2013) can be used as a criterion.

$$Accuracy = \frac{TP + TN}{TP + TN + FP + FN} \quad (1)$$

$$Sensitivity = \frac{TP}{TP + FN} \quad (2)$$

$$Specificity = \frac{TN}{TN + FP} \quad (3)$$

$$F - Measure = \frac{2TP}{2TP + TN + FB} \quad (4)$$

where TP is the number of true positives, TN is the number of true negatives, FP is the number of false positives, and FN is the number of false negatives.

## Results and discussion

The bone tumors were extracted, and other bones were removed. The calcaneal tumors' morphological parameters were shown in 3D (Figure 6).

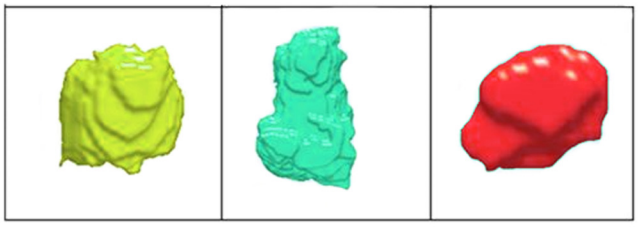

**Figure 6.** 3D modeling of tumors
**Source:** Authors

This study focused on automatic calcaneus tumor detection and diagnosis using CT. The results of radiologist reports were compared to those of CAD (Table 2).

**Table 2.** Comparison between morphological measurements and medical reports of 3D calcaneal tumors

| Patients | Our results (mm) | Radiologist reports (mm) |
|---|---|---|
| **1** | 20,65 x 16,11 | 22 (approximately) |
| **2** | 16,54 x 14,40 | 15 (approximately) |
| **3** | 6,25 x 8,99 | mm level |
| **4** | 29,10 x 21,97 | cystic structure |
| **5** | 43,03 x 26,35 | 40x25 |
| **6** | 57,86 x 45,98 | 40-50 (approximately) |
| **7** | 21,50 x 20,47 | 23x19 |
| **8** | 51,78 x 24,89 | cystic structure |
| **9** | 44,22 x 28,39 | cystic structure |
| **10** | 39,10 x 18,13 | cystic structure |

**Source:** Authors

Our method provides precise results, while medical reports provide approximate statements. The experimental results of the diagnostic performance metrics of the 3D process were evaluated with ROC. A threshold value of 0,5 was selected in the AUC plot. An ROC score of 80% and above is a good result. This study proposes an automatic segmentation method for automatic calcaneus tumor segmentation on CT images. Regarding the segmentation process, the average sensitivity, specificity, accuracy, and F-measure were 0,96%, 1,00%, 0,98, and 0,99%, respectively. The 3D method is computationally more complex than the 2D one, although interactive segmentation is highly accurate.

The standard radiological approach may be insufficient due to the irregular shapes of the anomalies that occur in the foot and ankle. Calcaneus tumors are rare (Young *et al.*, 2013) and the second most common tumor site in the foot (Kilgore and Parrish, 2005). Benign bone tumors are generally asymptomatic and go unexplored (Ladd and Roth, 2017). The lack of literature on calcaneal tumors is another compelling factor. Therefore, studies on detection are still insufficient, which constitutes a research gap. Defining and measuring the anomaly in a safe, metric, and reproducible manner can also be challenging for orthopedists (a radiological report is presented in Table 2). It is important to produce fast and reliable results.

This is an efficient technique to determine multiple anomalies in the slices. Benign bone lesions were more common than malignant ones. However, several limitations were noted in this study. Firstly, standardizing CT data could not be generated because they were obtained from a database. It is known that obtaining data under the same conditions and with similar characteristics increases the accuracy and reliability of a study. At the same time, the larger the number of datasets, the more accurate the generalization will be. Secondly, since more patients were needed, no distinction could be made between men and women. However, within the framework of this research, this distinction was observed on the last foot bones because images of healthy individuals were evaluated (Catal Reis, 2010). Thus, the error caused by the amount of data was kept to a minimum. However, computer-aided digital image processing applications have been employed in different fields. This method has some advantages, as it is time-saving, accurate, and economical (Tasdemir and Ozkan, 2018).

## Conclusions

The study used image processing, segmentation, clustering techniques, and modeling to detect foot bone tumors from CT images. All this, upon the basis of photogrammetry. This work examined the feasibility of computer-aided diagnosis for detecting foot bone tumors and tumor-like lesions in CT images and from 3D tumor models. The other contribution of this study was the design of an automatic method for 3D morphological measurements of bone tumors based on CT processing techniques. CAD for detecting calcaneus tumors of the foot can aid radiologists given its increased accuracy, sensitivity, specificity, and F-measure. Pre-processing applications can also increase the accuracy of 3D models.

The 3D reconstruction measurements based on image processing techniques were highly reliable and repeatable with regard to the anatomic and morphological measurement of the calcaneus. However, the limitations of our study include its small sample data size, different slice thicknesses,

and its retrospective design. Nevertheless, this technique will help to determine calcaneal tumors and tumor-like lesions. 3D foot bone cancer models can be developed using the approaches and future directions needed to advance these relatively new fields of research. Medical photogrammetry will continue to contribute to the literature as a second eye today and in the future. As future work, we aim to add machine and deep learning algorithms to our work and test them with different approaches.

### *Ethics approval and consent to participate*

Retrospective study/stock footage research.

### *Funding*

None.

### *Competing interests*

The authors declare that they have no competing interests.

## CRediT author statement

Hatice Catal Reis: conceptualization, methodology, software, validation, formal analysis, investigation, writing (original draft, writing, review, and editing), data curation. Bulent Bayram: Writing, editing, review, and validation.

## References

Aydın, M., and Kurnaz, T. F. (2023). An alternative method for the particle size distribution: Image processing. *Turkish Journal of Engineering, 7*(2), 108-115. https://doi.org/10.31127/tuje.1053462

Akcay, O., Erenoglu, R. C., and Avsar, E. O. (2017). The effect of jpeg compression inclose-range photogrammetry. *International Journal of Engineering and Geosciences*, *2*(1), 35-40. https://doi.org/10.26833/ijeg.287308

Bakotic, B., and Huvos, A. G. (2001). Tumors of the bones of the feet: The clinicopathologic features of 150 cases. *Journal of Foot & Ankle Surgery, 40*(5), 277-286. https://doi.org/10.1016/S1067-2516(01)80063-6

Basile, A. (2012). Subjective results after surgical treatment for displaced intraarticular calcaneal fractures. *Journal of Foot and Ankle Surgery, 51*, 182-186. https://doi.org/10.1053/j.jfas.2011.10.042

Bestic, J. M., Wessell, D. E., Beaman, F. D., Cassidy, R. C., Czuczman, G. J., Demertzis, J. L., Lenchik, L., Motamedi, K., Pierce, J. L., Sharma, A., Sloan, A. E., Than, K., Walker, E. A., Yung, E. Y. K., and Kransdorf, M. J. (2020). ACR appropriateness criteria: Primary bone tumors. *Journal of the American College of Radiology*, *17*(5S),S226-S238. https://doi.org/10.1016/j.jacr.2020.01.038

Campbell, C. J., and Leupold, R. G. (1973). Tumours and tumour-like conditions of the os calcis. *Orthopedic Clinics of North America, 4*,145-156. https://doi.org/10.1016/S0030-5898(20)30510-1

Catal Reis, H. (2010). *Metric analysis of orthopedic changes of ballerina's foot bones by photogrammetric techniques* [Master's thesis, Selcuk University]. http://acikerisimarsiv.selcuk.edu.tr:8080/xmlui/handle/123456789/660.

Catal Reis, H. (2018). Detection of foot bone anomaly using medical photogrammetry. *International Journal of Engineering and Geosciences*, *3*(1), 001-005. https://doi.org/10.26833/ijeg.333686

Costelloe, C. M., and Madewell, J. E. (2013). Radiography in the initial diagnosis of primary bone tumors. *American Journal of Roentgenology, 200*, 3-7. https://doi.org/10.2214/AJR.12.8488

Diémé, C., Dembélé, B., Gaye, A.M., Sarr, L., Coundoul, C., Gueye, A.B., Déme, H., Sané, A., and Seye, S. (2015). Osteosarcoma of the calcaneus: A case report. *Médecine et Chirurgie du Pied, 31*, 69-71. https://doi.org/10.1007/s10243-015-0407-1

Doğan, Y., and Yakar, M. (2018). GIS and three-dimensional modeling for cultural heritages. *International Journal of Engineering and Geosciences, 3*(2), 50-55. https://doi.org/10.26833/ijeg.378257

Eckstein, F., Cicuttini, F., Raynauld, J.P., Waterton, J.C., and Peterfy, C. (2006). Magnetic resonance imaging (MRI) of articular cartilage in knee osteoarthritis (OA): Morphological assessment. *Osteoarthritis and Cartilage, 14*(1), 46-75. https://doi.org/10.1016/j.joca.2006.02.026

Epstein. N., Chandran. S., and Chou. L. (2012). Current concepts review: Intra-articular fractures of the calcaneus. *Foot & Ankle International, 33*, 79-86. https://doi.org/10.3113/FAI.2012.0079

Esim A. K., Kaya, H., and Alcan, V. (2019). Determination of malignant melanoma by analysis of variation values. *Turkish Journal of Engineering, 3*(3), 120-126. https://doi.org/10.31127/tuje.472328

Foo, L. F., and Raby, N. (2005). Tumors and tumor-like lesions in the foot and ankle. *Clinical Radiology, 60*, 308-332. https://doi.org/10.1016/j.crad.2004.05.010

Gemescu, I. N., Thierfelder, K. M., Rehnitz, C., and Weber, M.-A. (2019). Imaging features of bone tumors conventional radiographs and MR imaging correlation. *Magnetic Resonance Imaging Clinics of North America*, *27*, 753–767. https://doi.org/10.1016/j.mric.2019.07.008

Ghafouri-Fard, S., Shoorei, H., and Taheri, M. (2020). Role of microRNAs in the development, prognosis and therapeutic response of patients with prostate cancer. *Gene, 759*, 144995. https://doi.org/10.1016/j.gene.2020.144995

González, R. C., and Woods, R. E. (2007). *Digital image processing* (2nd ed.). Publishing House of Electronics Industry.

Goodyear, M. D., Krleza-Jeric, K., and Lemmens, T. (2007). The declaration of Helsinki. *British Medical Journal, 335*, 624-625. https://doi.org/10.1136/bmj.39339.610000.BE

Gutekunst, D. J., Liu, L., Ju, T., Prior, F. W., and Sinacore, D. R. (2013). Reliability of clinically relevant 3D foot bone angles from quantitative computed tomography. *Journal of Foot and Ankle Research, 6*, 38. https://doi.org/10.1186/1757-1146-6-38

Hapani, H., Kalola, J., and Hapani, J. (2014). Comparative role of CT scan and MR imaging in primary malignant bone tumors. *IOSR Journal of Dental and Medical Sciences, 13*(11), 29-35. https://doi.org/10.9790/0853-131172935

Hasbek, Z., Salk, I., Yucel, B., Yucel, B., and Babacan, N. A. (2013). Which imaging method to choose for detection of bone metastases? Bone scintigraphy, CT, 18F-FDG PET/CT or MR? *Bozok Medical Journal, 3*(3),44-50. https://dergipark.org.tr/tr/download/article-file/43180

Hosseini, A., Mirzaei, A., Salimi, V., Jamshidi, K., Babaheidarian, P., Fallah, S., Rampisheh, Z., Khademian, N., Abdolbahavi, Z., Bahrabadi, M., Ibrahimi, M., Hosami, F., and Tavakoli-Yaraki, M. (2020). The local and circulating SOX9 as a potential biomarker for the diagnosis of primary bone cancer. *Journal of Bone Oncology, 23*, 100300. https://doi.org/10.1016/j.jbo.2020.100300

Kamal, F., Waryudia, A., Effendia, Z., and Kodrat, E. (2016). Management of aggressive giant cell tumor of calcaneal bone: A case report. *International Journal of Surgery Case Reports, 28*, 176-181. https://doi.org/10.1016/j.ijscr.2016.09.038

Kilgore, W. B., and Parrish, W. M. (2005). Calcaneal tumors and tumor-like conditions. *Foot and Ankle Clinics, 10*(3), 541-565. https://doi.org/10.1016/j.fcl.2005.05.002

Ladd, M. L., Roth, T. D. (2017). Computed tomography and magnetic resonance imaging of bone tumors. *Seminars in Roentgenology, 52*(4), 209-226. https://doi.org/10.1053/j.ro.2017.04.006

Lodwick, G. S., Haun, C. L., Smith, W. E., Keller, R. F., and Robertson, E. D. (1963). Computer diagnosis of primary bone tumors. *Radiology, 80*, 273-275. https://doi.org/10.1148/80.2.273

Mehta, K., McBee, M. P., Mihal, D. C., and England, E. B. (2017). Radiographic analysis of bone tumors: a systematic approach. *Seminars in Roentgenology, 52*(4), 194-208. https://doi.org/10.1053/j.ro.2017.04.002

Mistry, K. D., and Talati, B. J. (2016, Oct. 6-8). *Integrated approach for bone tumor detection from MRI scan imagery* [Conference presentation]. 2016 International Conference on Signal and Information Processing (IConSIP), Vishnupuri, India. https://doi.org/10.1109/ICONSIP.2016.7857471

Nahm, F.S. (2022). Receiver operating characteristic curve: overview and practical use for clinicians. Korean Journal of Anesthesiology, 75 (1), 25-36. https://doi.org/10.4097/kja.21209

Nishikawa, R. M. (2005). *Computer-assisted detection and diagnosis*. Wiley.

Nurtanio, I., Astuti, E. R., Purnama, I. K. E., Hariadi, M., Purnomo, M. H. (2013). Classifying cyst and tumor lesion using support vector machine based on dental panoramic images texture features. *IAENG International Journal of Computer Science, 40*, 1-4. https://www.iaeng.org/IJCS/issues_v40/issue_1/IJCS_40_1_04.pdf

Ozer, D., Aycan, O. E., Er, S. T., Tanritanir, R., Arikan, Y., and Kabukcuoglu, Y. S. (2017). Primary tumor and tumor-like lesions of bones of the foot: Single-center experience of 166 cases. *Journal of Foot & Ankle Surgery, 56*, 1180-1187. https://doi.org/10.1053/j.jfas.2017.05.027

Parker, E. R. (2021). The influence of climate change on skin cancer incidence – A review of the evidence. *International Journal of Women's Dermatology*, *7*(1), 17-27. https://doi.org/10.1016/j.ijwd.2020.07.003

Pirak, J., Brandeisky, J. A., Simon, P., and Khaladj, M. (2020). Elastofibroma in the rear foot: A case report of a rare soft tissue tumor. *Journal of Foot & Ankle Surgery, 59*, 587-589. https://doi.org/10.1053/j.jfas.2019.09.021

Plodkowski, A. J., Arimatei, J., Araujo-Filho, B., Simmers, C. D. A., Girshman, J., Raj, M., Zheng, J., Rimner, A., and Ginsberg, M. S. (2021). Pre-treatment CT imaging in stage IIIA lung cancer: Can we predict local recurrence after definitive chemoradiotherapy? *Clinical Imaging, 69*, 133-138. https://doi.org/10.1016/j.clinimag.2020.07.005

Qiang, M., Chen, Y., Zhang, K., Li, H., and Dai, H. (2014). Measurement of three-dimensional morphological characteristics of the calcaneus using CT image post-processing. *Journal of Foot and Ankle Research, 7*, 19. https://doi.org/10.1186/1757-1146-7-19

Reddy, K. K., Anisha, P. R., and Prasad, L. N. (2015). A novel approach for detecting the bone cancer and its stage based on mean intensity and tumor size. Medicine, *Recent Researches in Applied Computer Science*, 162-171. https://www.semanticscholar.org/paper/A-Novel-Approach-for-Detecting-the-Bone-Cancer-and-Reddy-Prasad/6214771aac055643a74a94a52287cb69dacbd2a8

Riis, M. (2020). Modern surgical treatment of breast cancer. *Annals of Medicine and Surgery, 56*, 95-107. https://doi.org/10.1016/j.amsu.2020.06.016

Scotto di Carlo, F., Whyte, M. P., and Gianfrancesco, F. (2020). The two faces of giant cell tumor of bone. *Cancer Letters, 489*,1-8. https://doi.org/10.1016/j.canlet.2020.05.031

Tasdemir, Ş., and Ozkan, I. A. (2019). ANN approach for estimation of cow weight depending on photogrammetric body dimensions. *International Journal of Engineering and Geosciences, 4*(1), 036-044. https://doi.org/10.26833/ijeg.427531

Toepfer, A. (2017). Tumors of the foot and ankle – A review of the principles of diagnostics and treatment. *Fuß & Sprunggelenk, 15*, 82-96. https://doi.org/10.1016/j.fuspru.2017.03.004

Yan, L., Zong, J., Chu, J., Wang, W., Li, M., Wang, X., Song, M., and Wang, S. (2018). Primary tumours of the calcaneus (Review). *Oncology Letters, 15*, 8901-8914, https://doi.org/10.3892/ol.2018.8487

Young, P. S., Bell, S. W., MacDuff, E. M., and Mahendra, A. (2013). Primary osseous tumors of the hind-foot: Why the delay in diagnosis and should we be concerned. *Clinical Orthopaedics and Related Research, 471*, 871-877. https://doi.org/10.1007/s11999-012-2570-6

Weilbaecher, K. N., Guise, T. A., and McCauley, L. K. (2011). Cancer to bone: A fatal attraction. *Nature Reviews: Cancer, 11*, 411-425. https://doi.org/10.1038/nrc3055

Zilberman, Y., and Sonkusale S. R. (2015). Microfluidic optoelectronic sensor for salivary diagnostics of stomach cancer. *Biosensors and Bioelectronics, 6715*, 465-471. https://doi.org/10.1016/j.bios.2014.09.006